



HAL
open science

Microplastics in different water samples (seawater, freshwater, and wastewater): Methodology approach for characterization using micro-FTIR spectroscopy

J. Yang, M. Monnot, Y. Sun, L. Asia, P. Wong-Wah-Chung, P. Doumenq, P. Moulin

► To cite this version:

J. Yang, M. Monnot, Y. Sun, L. Asia, P. Wong-Wah-Chung, et al.. Microplastics in different water samples (seawater, freshwater, and wastewater): Methodology approach for characterization using micro-FTIR spectroscopy. *Water Research*, 2023, 232, pp.119711. 10.1016/j.watres.2023.119711 . hal-04055825

HAL Id: hal-04055825

<https://hal.science/hal-04055825>

Submitted on 16 Feb 2024

HAL is a multi-disciplinary open access archive for the deposit and dissemination of scientific research documents, whether they are published or not. The documents may come from teaching and research institutions in France or abroad, or from public or private research centers.

L'archive ouverte pluridisciplinaire **HAL**, est destinée au dépôt et à la diffusion de documents scientifiques de niveau recherche, publiés ou non, émanant des établissements d'enseignement et de recherche français ou étrangers, des laboratoires publics ou privés.

1 **Microplastics in different water samples (sea, fresh and wastewater) - Part**
2 **I: methodology approach for characterization using micro-FTIR spectroscopy**

3 *J. Yang¹, M. Monnot¹, Y. Sun¹, L. Asia², P. Wong-Wah-Chung², P. Doumenq², P. Moulin^{1*}*

4 (1) Aix Marseille Univ, CNRS, Centrale Marseille, M2P2, Equipe Procédés Membranaires (EPM),
5 Marseille, France

6 (2) Aix Marseille Univ, CNRS, LCE, Marseille, France

7 *Correspondence: philippe.moulin@univ-amu.fr; Tel.: +33 6 67 14 14 18

8
9 **Abstract:**

10 Microplastics of millimeter dimensions have been widely investigated in environmental
11 compartments and today, studies are mainly focused on particles of smaller dimensions (µm-nm).
12 However, as there are no relevant standards or policies for the preparation and analysis of water
13 samples containing such particles, the results may be questionable. Therefore, a methodology
14 approach for 10 µm to 500 µm microplastics analysis was developed using µ-FTIR spectroscopy
15 coupled with the siMPle analytical software. This was undertaken on different water samples (sea,
16 fresh and wastewater) considering rinsing water, digestion and filtration step and sample
17 characteristics. Ultrapure water reveals to be the optimal rinsing water and ethanol was also
18 proposed with a mandatory previous filtration. This improved quantitative and qualitative
19 analytical methodology for microplastics detection by µ-FTIR spectroscopy will be used in Part II
20 to assess the removal efficiency of conventional and membrane treatment processes in different
21 water treatment plants.

22
23 **List of abbreviations**

24

Abbreviation	Full name
ABS	Acrylonitrile Butadiene Styrene
ATR	Attenuated total reflection
DWTP	Drinking water treatment plant

EVA	Ethylene Vinyl Acetate
FTIR	Fourier-transform infrared
IC	Inorganic carbon
MCT	Mercuric cadmium telluride
MP	Microplastic particle
PA	Polyamide (nylon)
PE	Polyethylene
PES	Polyether Sulfone
PET	Polyethylene Terephthalate
PP	Polypropylene
PS	Polystyrene
PVC	Polyvinyl Chloride
SWTP	Seawater treatment plant
TOC	Total organic carbon
TC	Total carbon
TP	Total particles
UF	Ultrafiltration
UP	Ultrapure
WWTP	Wastewater treatment plant

25

26 1. Introduction

27 Researches on microplastics sources, pollution, transport, harmfulness, retention, recovery and
28 analytical methods have been increasingly developed for the last 10 years. Microplastic particles
29 (MPs) (0.1 μm ~ 5 mm) are originated either from primary manufactured or secondary degraded
30 plastic objects (Frias and Nash, 2019). Annually in Europe, polymers production was increased
31 greatly from 0.35 million tons in the 1950s to 55 million tons in 2020, while 63,000 to 430,000
32 tons of microplastics enter farmland through compost/sludges application (Nizzetto et al., 2016),
33 and around 2,461~8,627 tons of microplastics enter in marine environments (Jambeck et al., 2015;
34 Lebreton et al., 2017; C. Sherrington et al., 2016). Massive MP caused increasing adverse effects
35 on humans and environments: (1) MPs can be swallowed by organisms and transported through
36 food chains (Rillig, 2012). For instance, Ragusa et al., (2021) discovered the presence of

37 microplastics (5~10 μm) in human placenta, and Sussarellu et al., (2016) found polystyrene (PS)
38 particles (2 ~ 6 μm) translocated in blood circulation and cause reproductive disruption for marine
39 filter feeders; (2) Some MPs could release toxic compounds such as dioxins, phthalates, vinyl
40 chloride, etc. Some additives added by manufacturers such as plasticizers, stabilizers and pigments
41 to plastics, are mostly hazardous substances (Nobre et al., 2015); (3) MPs could induce chronic
42 toxicity which was considered as a key issue for long-term exposure (Campanale et al., 2020; Prata
43 et al., 2019); (4) MPs could act as vectors for toxic organic substances and microorganisms (Nobre
44 et al., 2015; Yang et al., 2022); (5) Moreover, old microplastics could be furtherly degraded into
45 smaller or even nanoparticles (Jambeck et al., 2015). Currently, public perception of the risks
46 induced by microplastics is low, and few countries or regions have issued relevant detection
47 method standards and production/limitation policies.

48 Among present analytical methods, micro-FTIR (μ -FTIR) spectroscopy is an advanced
49 analytical approach for testing MPs. It is a non-destructive analytical technique and can produce
50 IR absorption spectra for both thick and opaque materials (Hong et al., 2021; Shim et al., 2017).
51 Generally, the requirement for sample pretreatment is necessary for avoiding shelter of
52 microplastics by organic and inorganic materials and allow their indubitable identification by
53 digestion. The common digestion protocols include oxidation, alkaline or acidic treatment, and
54 enzymatic degradation (Stock et al., 2019; Sun et al., 2019). H_2O_2 and Fenton reagent are mostly
55 used chemicals for oxidative digestion, which generates no or very few effects on microplastic
56 properties (Hurley et al., 2018; A. Tagg et al., 2015). According to Prata et al. (2019), 95% of 20
57 studies in sediments used H_2O_2 and/or Fenton reagent for digestion, and >60% of 20 studies in
58 water samples used H_2O_2 for digestion. Similar conclusion was also inferred in the survey of
59 Table S1 (supplementary information, SI). In comparison, Fenton reagent is able to accelerate
60 digestion rates compared to H_2O_2 (Hurley et al., 2018). Alkaline digestion with 10% KOH solution
61 is highly recommended for sea animals or sea water digestion since it can break down soft tissue
62 and bivalve tissues in marine samples (Thiele et al., 2019). KOH is also useful on the digestion of
63 natural organic matters, feathers, and fat, etc. Enzymatic digestion is a rapid reaction for complete
64 degradation of organics, while it is considered as an expensive, complex, and sometimes
65 destructive method on MPs extraction (Prata et al., 2019). Density separation with salt of NaCl,
66 NaI, and ZnCl_2 could be coupled with other digestion processes to isolate MPs (J. Li et al., 2018),
67 but showed lower recovery on smaller and denser MPs (Radford et al., 2021). Currently, the

68 digestion protocols on microplastics recovery are mostly based on experiments from literature, the
69 preparation methods are not yet standardized. In view of rinsing process, most studies used
70 ultrapure water with or without ethanol (66.7% of 30 studies), secondly used distilled water by
71 investigation in SI Table S2. Since particles from rinsing could easily stick to surfaces and remain,
72 thus would lead to contamination of the sample, certain criteria need to be met for rinsing: 1)
73 evaluating the MPs existence in potential rinsing water/solution and potentially filtrate it before
74 using; 2) determining the reliable rinsing water/solution with minimum MPs before experiments.
75 However, fewer studies completed the above steps, thus it is necessary to investigate the MPs in
76 rinsing water/solution to avoid external invasion. Additionally, considering the expression of
77 MPs concentration, fewer researchers filtrated 1 L of samples for analysis while others,
78 particularly for organic-rich samples, maybe filtrated only several milliliters (Simon et al., 2018).
79 Most of them calculated MPs concentration by assuming the proportional relationship between the
80 filtrated volume and the MPs counts but without evidencing it.

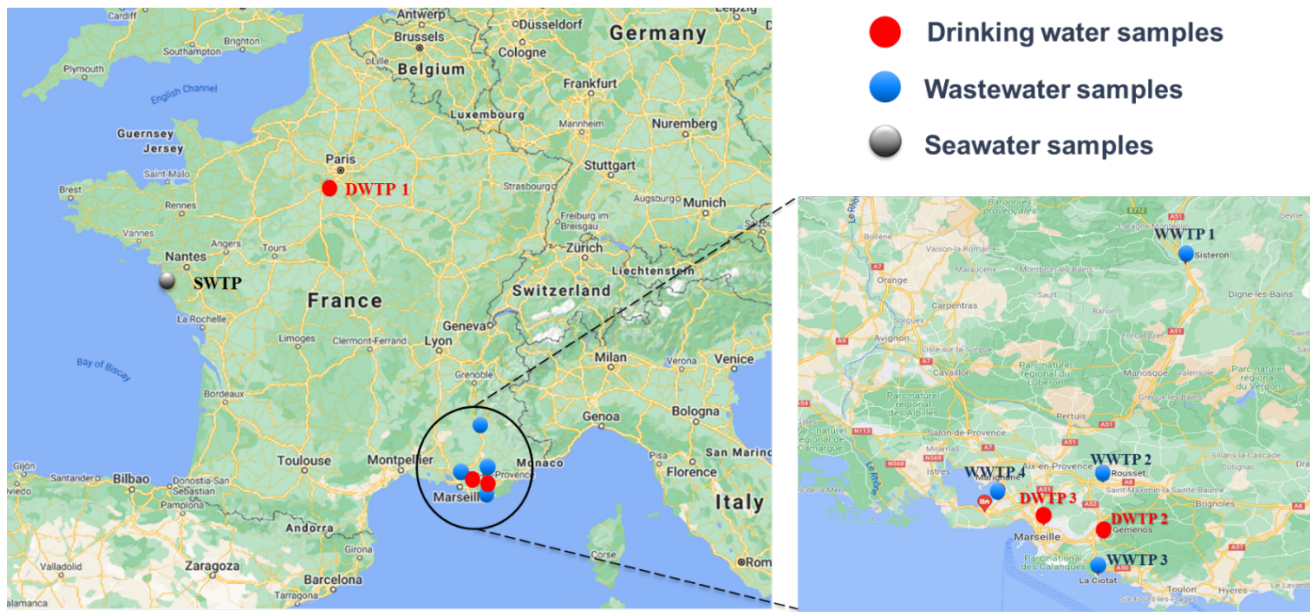
81 Therefore, current difficulties on MPs analysis include the incomplete recovery of MPs from
82 samples, the selection of appropriate digestion method *vs.* nature of samples, the limitation on
83 quantification and identification of MPs, and the global accuracy of analytical results. Therefore,
84 this study aims to develop a method for identification (type and size) and quantification of MPs in
85 different water samples. Efforts have been made on the improvement of detection accuracy:
86 selection of purified rinsing water, suitable sampling and digestion methods depending on the
87 water type, rigorous detection process, and high-precision analytical methods to obtain the counts,
88 dimensions, and type of microplastics by μ -FTIR in reflectance mode.

89 2. Material and methods

90 2.1. Sample sources

91 Three types of water were analyzed and their location was shown in Figure 1: (i) samples from
92 a seawater treatment plant (SWTP) which aims to treat seawater before shellfish farms to produce
93 purified seawater; (ii) samples from four different wastewater treatment plants (WWTP); and (iii)
94 samples from 3 drinking water treatment plants (DWTP). The detailed information of each site is

95 shown in Table 1. To avoid external pollution, all samples were collected and transported via 1 L
 96 glass bottles and frozen up until analysis.



97
 98 Figure 1 Locations and types of sampling in France (background map from Google Map © 2022)

99 Table 1 Information of water treatment plants

Types	Names	Samples	Main process (studied in Part II)	Location in France (French department)	Sampling date
Wastewater	WWTP 1	Pharmaceutical membrane bioreactor (MBR) feed and effluent	MBR (0.02 μm UF)	Alpes-de-Haute-Provence	April 2021
	WWTP 2	Municipal wastewater and secondary effluents	MBR (0.1 μm UF)	Bouches-du-Rhône	October 2021
	WWTP 3		Physico-chemical with biofiltration	Bouches-du-Rhône	October 2021
	WWTP 4		Activated sludge, 200 kDa UF	Bouches-du-Rhône	October 2021
Seawater	SWTP	Seawater and secondary/tertiary effluents	Zeolite, filters, 200 kDa UF	Vendée	April 2021
Drinking water	DWTP 1	Underground water and effluents	Sieves, 200 kDa UF	Paris	September 2021
	DWTP 2	Surface water and effluents	200 kDa UF	Bouches-du-Rhône	October 2021
	DWTP 3	Surface water and effluents	Sedimentation, sand filtration	Bouches-du-Rhône	October 2021

100

101

102 2.2. Sample pretreatment

103 The commonly used rinsing water/solutions tested in this study included Evian water, ultrapure
104 water (UP water) (LaboStar TWF7 Siemens), distilled water (DI), tap water, HPLC water (34877-
105 2.5L-M, Sigma Aldrich), and ethanol both in PE and glass bottles (ethanol absolute, VWR, USA).
106 The digestion chemicals used for samples included 30% (w/v) H₂O₂ (Fisher Chemical), 10% (w/v)
107 KOH (Fischer Chemicals), 1–10% H₂SO₄ (>95%, Fisher Scientific), and Fenton reaction
108 (0.05 M FeSO₄·7H₂O with 30% H₂O₂ at volume ratio of 1:1). FeSO₄·7H₂O solution was made by
109 dissolving 2.5 g of FeSO₄·7H₂O (Fisher Scientific) in 165 mL UP water and acidified with 1 mL
110 of concentrated H₂SO₄. All operations were conducted in cleaned glass devices and covered with
111 aluminum foil to prevent airborne contamination. Digestion processes were all operated at room
112 temperature (25 °C). The handling of samples was carried out under controlled air conditions in
113 cleaned fume hood, and operators wore cotton laboratory coats throughout the experiment.

114 Turbidity of water samples was measured using WTW Turb 550 IR in Nephelometric Turbidity
115 Unit (NTU). Total Organic Carbon (TOC) was measured using Shimadzu TOCL-LCSH/CSN
116 TOC Analyzer. Detailed information was shown in SI Section 1.1.

117 2.3. MPs collection

118 The final step before μ -FTIR imaging was the filtration of samples. Three types of filters were
119 used: 3 or 5 μ m gold-coated polyester membranes (i3 TrackPor P, Germany), and 25 μ m stainless-
120 steel filters. In reflectance mode, the gold material and stainless-steel slide were both good choices
121 as background as they reflected IR radiation with less absorption (Gonzalez-Torres et al., 2017).
122 The samples were filtrated through a vacuum Büchner funnel apparatus (Fisher Scientific,
123 Sweden), shown in Figure S1. The filtration masks were round metal discs with a square hole in
124 the center to regulate the sedimentation area on filters. Square holes with side dimension of 5,500
125 and 10,000 μ m, were respectively used on gold-coated filters and stainless steel filter. For samples
126 with visible particles and solids, a two-stage filtration was performed: Step 1 by stainless-steel
127 filter, step 2 by gold filter. For purified water samples, the filtration was directly achieved on a
128 gold filter. Before and after analysis by μ -FTIR spectroscopy, the filter with collected sample was
129 stored in a glass Petri dish to avoid any external pollution.

130 2.4. μ -FTIR spectroscopy

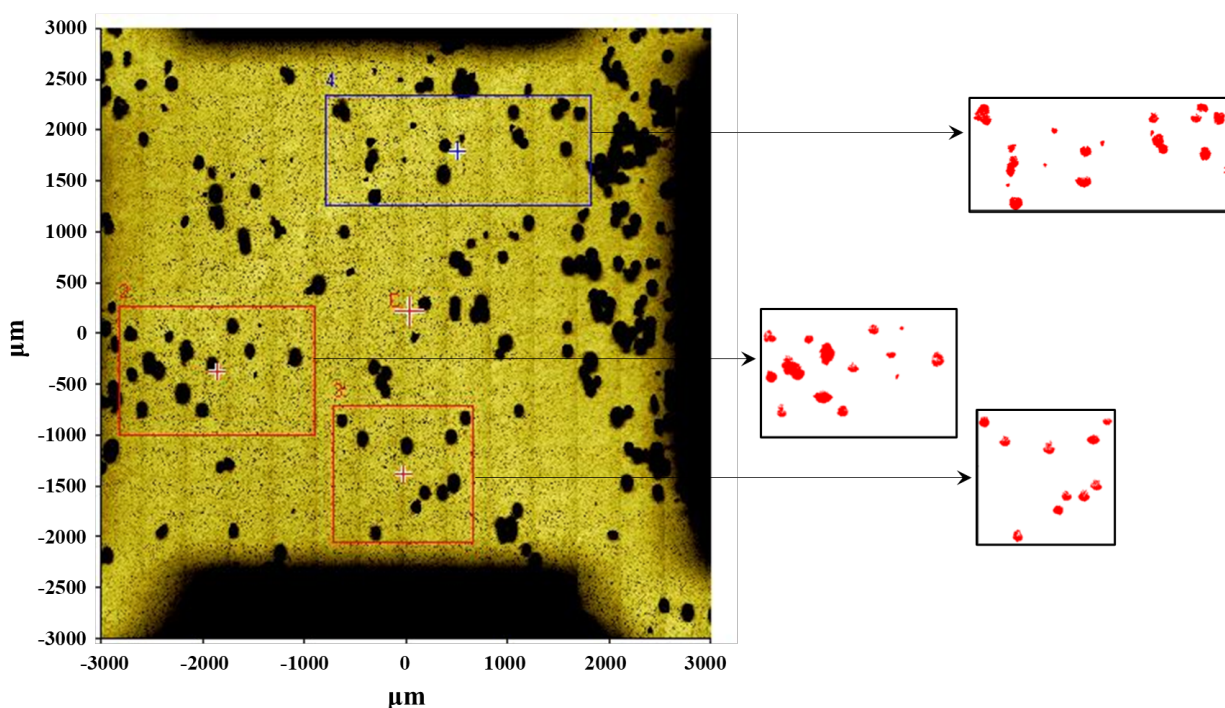
131 The detection of microplastics was achieved with the μ -FTIR imaging system Spotlight 400 M-
132 FTIR microscope (PerkinElmer, USA) with high sensitivity on smaller particles ($<10 \mu\text{m}$). The
133 detailed information was described in SI section 1.2. In this study, the spectrometer was set up to
134 reflectance mode with a focal-plane-array detector which assembly enabled rapid analysis of thick
135 and opaque samples such as microplastics (A. S. Tagg et al., 2015). A 16 cm^{-1} spectral resolution
136 was used as the best compromise between spectral quality and acquisition rapidity (Zheng et al.,
137 2021). A background spectrum imaging was collected from the gold filter both at $6.25 \mu\text{m}$ or 25
138 μm pixels. The other identification parameters of μ -FTIR are: 2 scans per pixel, an interferometer
139 velocity of $2.2 \text{ cm}\cdot\text{s}^{-1}$, IR spectral range of $4,000 \text{ cm}^{-1}$ – 690 cm^{-1} , and imaging resolution of 6.25
140 μm or $25 \mu\text{m}$ was selected depending on the filters. For each sample, the μ -FTIR generated an
141 absorbance image ($<1.5\text{h}$ duration per filter) with an infrared spectrum information on each pixel.

142 2.5. siMPle for Rapid Identification and Quantification of Microplastics

143 To identify microplastics' structures in this study, a freeware, siMPle, developed by Aalborg
144 University, Denmark and Alfred Wegener Institute, Germany (<https://simple-plastics.eu/>), was
145 adopted. The reference database contains most polymers and natural materials such as protein and
146 cellulose, a total of 23 material types. Primpke et al. (2020) verified the high sensitivity and high
147 accuracy for microplastic identification by siMPle, with $> 95\%$ correct assignment rates on spectra.
148 siMPle provided polymer types, range of abscissa and ordinates, number of pixels, minor/major
149 dimensions, surface area, and estimated volume and mass of each particle. In this study, MPs
150 concentrations were expressed ($\text{MP}\cdot\text{L}^{-1}$) and surface area ($\mu\text{m}^2\cdot\text{L}^{-1}$) was also provided to better
151 understand the 2D structure of particles. The estimated 3D data in the detection system, such as
152 mass ($\text{mg}\cdot\text{L}^{-1}$) and volume ($\mu\text{m}^3\cdot\text{L}^{-1}$), were not used because the thickness and shapes of particles
153 were both calculated by empirical assumption in previous studies (Minténig et al., 2020; Simon et
154 al., 2018).

155 2.6. Verification of type and dimensions of polyethylene microspheres and of
156 proportionality between quantity of MP and water volume

157 Synthetic polyethylene (PE) microspheres ($0.96 \text{ g}\cdot\text{cm}^{-3}$; $10 \text{ }\mu\text{m}$ - $150 \text{ }\mu\text{m}$) from Cospheric, USA
158 were used as referred MPs. Moreover, due to their hydrophobic properties, PE particles were
159 oxidized under UV light for 5 days (400 W , $60 \text{ }^\circ\text{C}$ in SEPAP 12–24, Atlas), and their spectra were
160 not changed by FTIR-ATR verification, to evenly distributed in UP water. The μ -FTIR images of
161 PE microspheres were shown in Figure 2. Statistical data analysis was performed using Microsoft
162 Office Excel 2016 and SPSS (version 22, SPSS Inc.). The test for normal distribution uses Shapiro
163 Wilk test on distribution of particle dimensions and showed that both minor dimensions (d_{min}) and
164 major dimensions (d_{maj}) of PE fitted with a normal distribution (normality test, $p > 0.05$), resulting
165 in $50 < d_{\text{min}} < 100 \text{ }\mu\text{m}$ and $100 < d_{\text{maj}} < 150 \text{ }\mu\text{m}$, respectively.



166

167 Figure 2 Visible survey and image of PE microspheres under μ -FTIR

168 To confirm whether the filtrated volume and the MPs counts is positively related, two
169 experiments were designed to investigate: 1) MPs concentration in different volumes (250 , 500 ,
170 $1,000$ and $2,000 \text{ mL}$) of UP water and 2) PE_MPs concentration in different volumes (250 , 500 ,
171 $1,000$ and $2,000 \text{ mL}$) of synthetic PE suspension ($0.1 \text{ mg}\cdot\text{L}^{-1}$). $0.1 \text{ mg}\cdot\text{L}^{-1}$ PE suspension was made

172 from a 10 mg·L⁻¹ PE stock solution which has been stirred ≥ 1 h before sampling. The synthetic
173 PE suspensions were also stirred for 1 h and sonicated for 15 min before filtration. Each sample
174 was detected in 3 replicates, and all filtrated through the 5µm gold-coated filters. The PE_MPs
175 concentration in synthetic PE suspensions excluded the number of PE in UP water. The coefficient
176 of MPs concentration in different volumes was calculated based on Eq(1):

$$177 \quad E = (1 - C_{\text{MPs}} / C_{\text{MPs-Ave}}) \times 100\% \quad \text{Eq(1)}$$

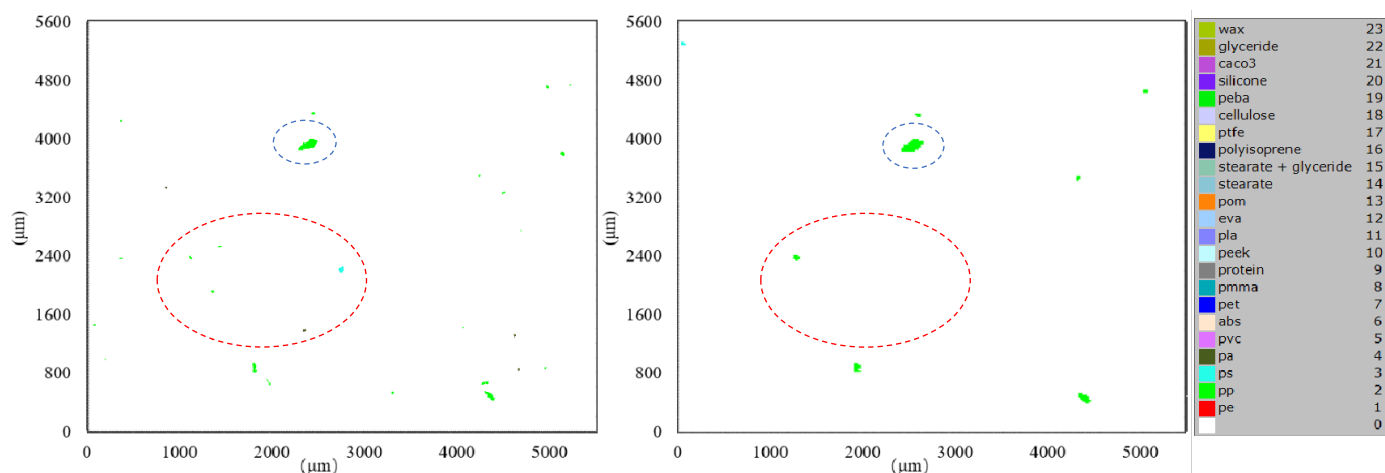
178 Where C_{MPs} (MP·L⁻¹) represents the tested MPs concentration in samples; $C_{\text{MPs-Ave}}$ (MP·L⁻¹)
179 represents average MPs concentration in effective samples. A one-way analysis of variance
180 (ANOVA) was conducted for linear regression test on particle numbers. All tests were statistically
181 verified with $p < 0.05$.

182 3. Results

183 3.1. Identification and quantification of microplastic particles by µ-FTIR and siMPle

184 To obtain high-qualified results, differences between two imaging resolutions of µ-FTIR (6.25
185 µm and 25 µm) was investigated. As the maximum pore size of filters used was 25 µm, the
186 oversized resolution of 50 µm was not considered in this study. Figure 3 showed the spectra maps
187 of MPs and total particles (TPs), including MPs and natural particles, on the same sample (1L DI
188 water collected on 3 µm filter) under 6.25 µm and 25 µm resolutions imaging. The results showed
189 that: imaging at 6.25 µm resolution quantified 713 TPs, 31 MPs with types of PP, PA and PS;
190 while imaging at 25µm resolution quantified only 407 TPs, 9 MPs with types of PP and PS on the
191 filter. In Figure 3, the position, shape, and material types of most particles at 25 µm resolution
192 were consistent to that at 6.25 µm resolution. While, higher resolution, 6.25 µm, exhibited more
193 precise identification and quantification of MPs by µ-FTIR compared to lower resolution (25 µm):
194 1) lower resolution showed larger dimensions/surface area than higher resolution (blue dotted
195 circle); 2) lower resolution might fail to capture smaller particles (red dotted circle); 3) lower
196 resolution showed weaker quantification of closer particles which may be considered as one big
197 particle (black dotted circle); 4) lower resolution identified less materials of particles. In contrary,
198 higher resolution usually consumed longer detection time and larger space for storage, imaging at

199 6.25 μ m took almost 16 times longer than at 25 μ m. Similar results were also exhibited in other
 200 samples, such as Tap water (SI Figure S2).

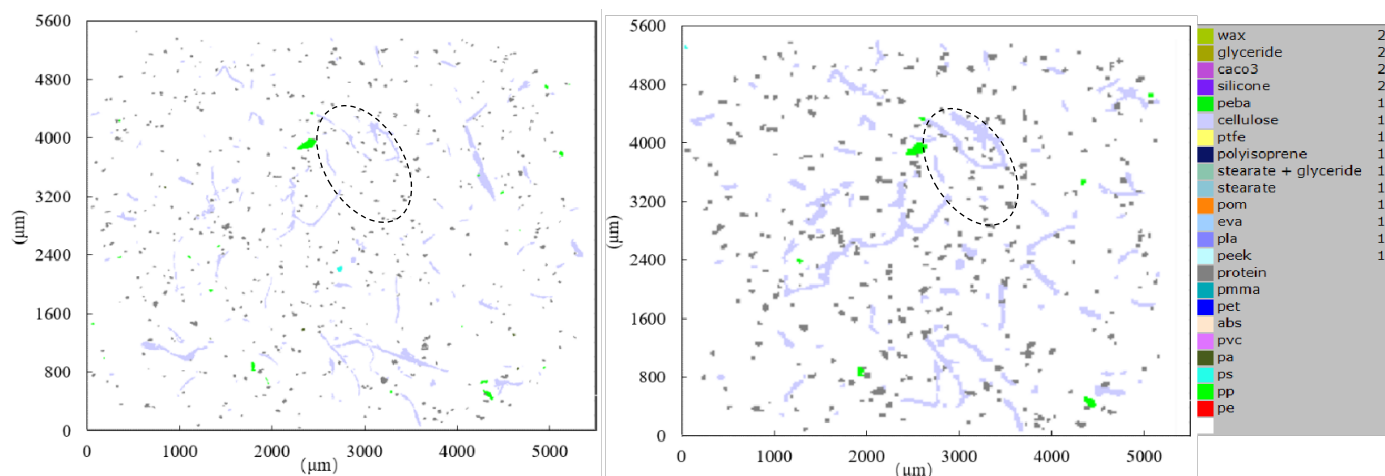


201

(a) MP_6.25 μ m

(b) MP_25 μ m

202



203

(c) TPs_6.25 μ m

(d) TPs_25 μ m

204

205 Figure 3 Spectra map of only MPs and TPs in distilled water from siMPle: (a) (b) represents MPs image
 206 by μ -FTIR at 6.25 μ m and 25 μ m resolution, respectively; (c) (d) represents TPs image by μ -FTIR at 6.25
 207 μ m and 25 μ m resolution, respectively.

208

209 Considering the pros and cons, resolution of 6.25 μ m was the dominant detection for all samples,
 210 and imaging at 25 μ m was just recommended when the pore size of filters were ≥ 25 μ m, with

211 shorter detection time and larger storage space. In this study, the image on 25 μm filters used the
212 25 μm resolution, and the image on 3 or 5 μm filters used 6.25 μm resolution.

213 3.2. Filtration apparatus efficiency and rinsing selection.

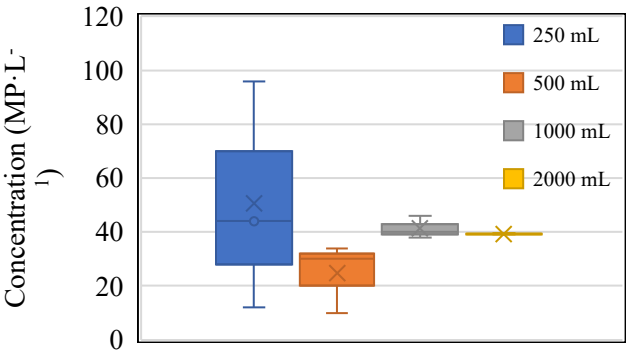
214 Table 2 showed the abundances, types, and dimensions of MPs and TPs in different types of
215 rinsing water by 6.25 μm imaging. Air quality was tested by filtrating air by vaccum pump for 30
216 min at 80 kPa, with 46 TPs and 2 PE MPs detected, confirming the ignorable influence of air on
217 MPs results. The filtration of all water samples (1 L) through the gold-coated filter (5 μm) was
218 rapid (< 30 s) and replicated ($n \geq 3$).

219 In result, ethanol either in glass or PE bottles contains hundreds of MPs (most in PE) thus was
220 not recommended for rinsing directly. DI water was secondly ranked in MPs concentration, while
221 HPLC water exhibited the lowest concentration. The MPs concentrations in Evian, tap water, and
222 UP water were ranged in the middle, while UP water contained the lowest TPs. Since DI and UP
223 water were both generated from tap water, the increase MPs concentration and MPs types (PET,
224 silicone, or EVA) might be related to process contamination by polymer pipes, taps, or filters, and
225 the purified process was contributed to TPs removal. Considering the pros and cons, the following
226 water/solution was not applied for rinsing in this study: tap and DI water excluded due to large
227 amount of TPs, untreated ethanol due to abundant MPs; HPLC water due to expensive cost.; and
228 Evian water due to the considerable cost and the presence of large particles (d_{maj} :20-200 μm ;
229 d_{min} :16-100 μm). In this study, UP water and purified ethanol (< 5 MPs filtrated by 0.22 μm
230 membrane) were used for rising. As UP water was selected due to acceptable MPs concentration,
231 the lowest quantity of TP, and smaller dimensions of MPs; filtrated ethanol was recommended due
232 to with its merits on both hydrophilicity and lipophilicity. Ethanol was suggested to be prefiltered
233 through a $< 1\mu\text{m}$ of non-plastic membranes to control the microplastics abundance before use.
234 Additionally, the volume of rinsing water was controlled within $< 50\text{mL}$ ($\approx 1.0 \pm 0.4$ MPs) which
235 caused ignorable influences on MPs results.

236

237

238



Types in bold and TPs in *italics*), types and minor and major dimensions of MP in different rinsing solutions

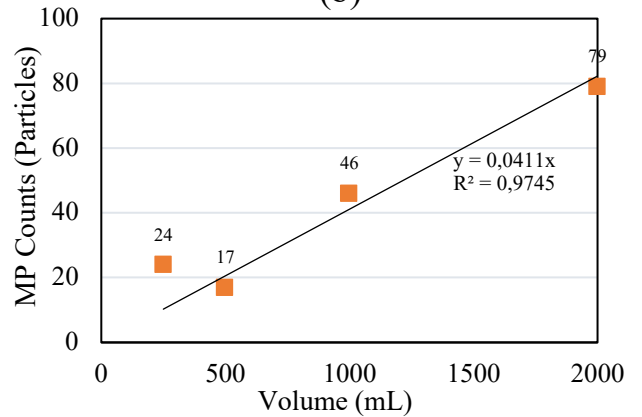
		Types	Major dimension of MP (µm)	Minor dimension of MP (µm)
		PE, PP, PS, PA, PET, PVC, Silicone	20-150	10-60
DI Water	26 ± 10 <i>558 ± 239</i>	PA, PP, PS, PET, PVC, ABS, PE, EVA, Silicone	20-250	10-120
Evian	8 ± 7 <i>350 ± 146</i>	PA, PE, PP, PS, PET	20-200	16-100
Tap water	6 ± 3 <i>1410 ± 156</i>	PS, PA, PP, PVC	45-80	10-40
HPLC grade water	1 <i>361</i>	PP	25-64	13-28
Ethanol in glass bottle	202 <i>526</i>	PE, PP, PET, PA, PS	20-304	13-112
Ethanol in PE bottle	304 ± 70 <i>1317 ± 445</i>	PA, PE, PET, PP, PS	15-488	7-177

241

242 3.3. Abundance and Distribution of MPs vs. Volume Analyzed

(a)

(b)

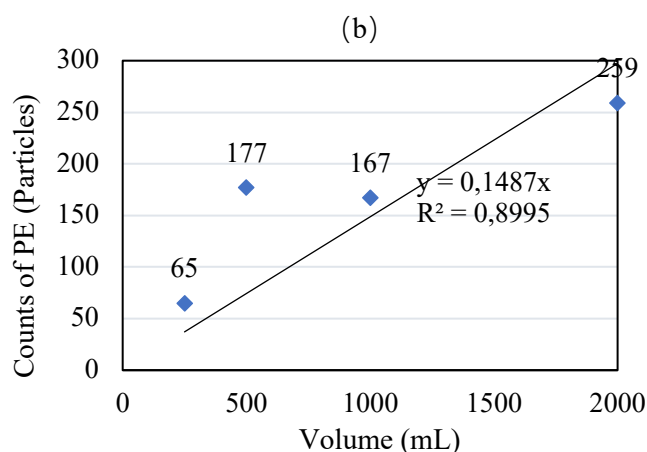
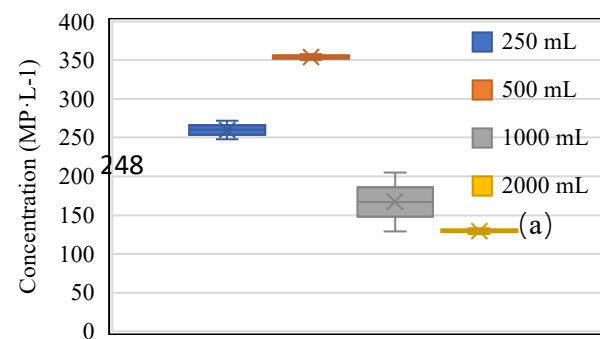


243

244 Figure 4 (a) MPs concentration (theoretically constant) versus different volumes of UP water in Box Plot
 245 and (b) linear regression of MPs counts versus UP volume

246

247



249

250 Figure 5 (a) PE_MPs concentration (theoretically constant) versus volumes of PE suspension ($0.1 \text{ mg}\cdot\text{L}^{-1}$
 251 ¹) in Box Plot and (b) linear regression of PE counts versus filtrated volume

252 In UP water, the statistical test showed a positive correlation between MPs concentration and
 253 filtrated volume ($p = 0.004 < 0.05$, $R^2 = 0.9745$), shown in **Erreur ! Source du renvoi introuvable.**
 254 In **Erreur ! Source du renvoi introuvable.**(a), MPs concentration tended to stabilize when
 255 filtering volume ≥ 500 mL which was consistent with the results obtained by Prata et al. (2020).
 256 The coefficient of variation decreased with increasing filtrated volume, resulting in 13.6% (500mL)
 257 \rightarrow 11.9% (1000mL) \rightarrow 3.8% (2000mL). In MPs-enriched suspension in Figure 5, PE_MPs
 258 concentration versus volumes of $0.1 \text{ mg}\cdot\text{L}^{-1}$ PE synthetic suspensions resulted in positive
 259 correlations ($p = 0.038 < 0.05$, $R^2 = 0.8995$), as expected. Moreover, PE_MPs concentration tended
 260 to stabilize when filtering volume ≥ 1000 mL. As a result, it can be inferred that MPs concentration
 261 was definitely positive-related with filtrated volumes. Particularly, both UP water and PE synthetic
 262 suspensions did not contain organic matters, therefore, poor-organic samples with volumes \geq
 263 500 mL were considered as an optimum compromise between drawbacks and reliability of results.

264 However, samples in actual conditions may contain thousands or millions of MPs per liter and
 265 be rich in organics while impossible to complete by one-time detection. According to Anger et al.
 266 (2018) and Karlsson et al. (2020), MPs counts in subsamples fitted with continuous Gaussian
 267 distribution when samples with higher level of contamination, thus subsamples provided higher
 268 probability of accuracy. Being more precise, it is necessary to take subsamples with smaller
 269 volume (< 500 mL) but more replicates (4~10 times) to improve the accuracy and reliability of

270 results. Accordingly, samples in this study were separated into two groups: poor-organic samples
271 (once filtrated volume $\geq 500\text{mL}$) and rich-organic samples (once filtrated volume $< 500\text{mL}$). To
272 be rigorous, poor-organic samples were tested with volume of 500~1000mL once and with 2-3
273 replicates; rich-organic samples were tested with the proper volume ($<500\text{mL}$) once and with 4-
274 10 replicates to increase the reliability of samples (shown in Table 3).

275 3.4. Digestion protocol

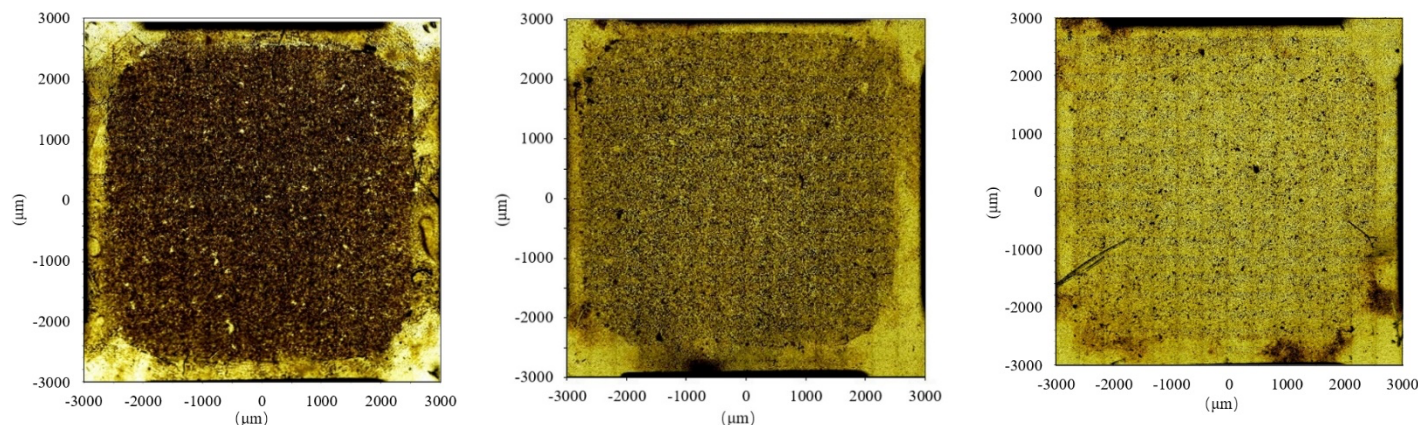
276 In this study, transparent samples with no visible suspended particles that were not digested and
277 thus directly filtrated, including tap water, DI water, ultrapure water, Evian water, HPLC water,
278 ethanol, tertiary treated effluents from DWTPs, WWTPs and SWTPs such as UF permeate, 1 and
279 $0.2\ \mu\text{m}$ outlets. Otherwise, for other samples (from DWTPs, WWTPs and SWTPs), a digestion
280 process was necessary. The choice of digestion methods in different samples was explored and
281 discussed in the following sections. The thoroughness of the digestion was closely related to
282 temperature, dose of chemicals, and reaction duration. In this study, the dose of chemicals was
283 added based on the literature experiments and testing in the lab.

284 3.4.1. Digestion of samples from WWTPs with H_2O_2 and Fenton

285 In view of secondary effluents from WWTPs, secondary effluents usually caused dense fouling
286 on gold-coated filters which was unusable by IR spectroscopy.

287 Figure 6 (a) showed the filter image filtrated with 50 mL secondary effluent from WWTP 4,
288 resulting in severe dark fouling cake digested by 1d H_2O_2 . In following 7–10 d, the filter became
289 cleaner with reaction time (

290 Figure 6 (b) (c)). Similar results were appeared on other WWTPs, digestion with 30% H_2O_2
291 ($V_{\text{sample}}:V_{\text{H}_2\text{O}_2}=1:2$) for 3-10d showed effective oxidation effects on all secondary effluents from
292 WWTPs, as shown in Table 3.



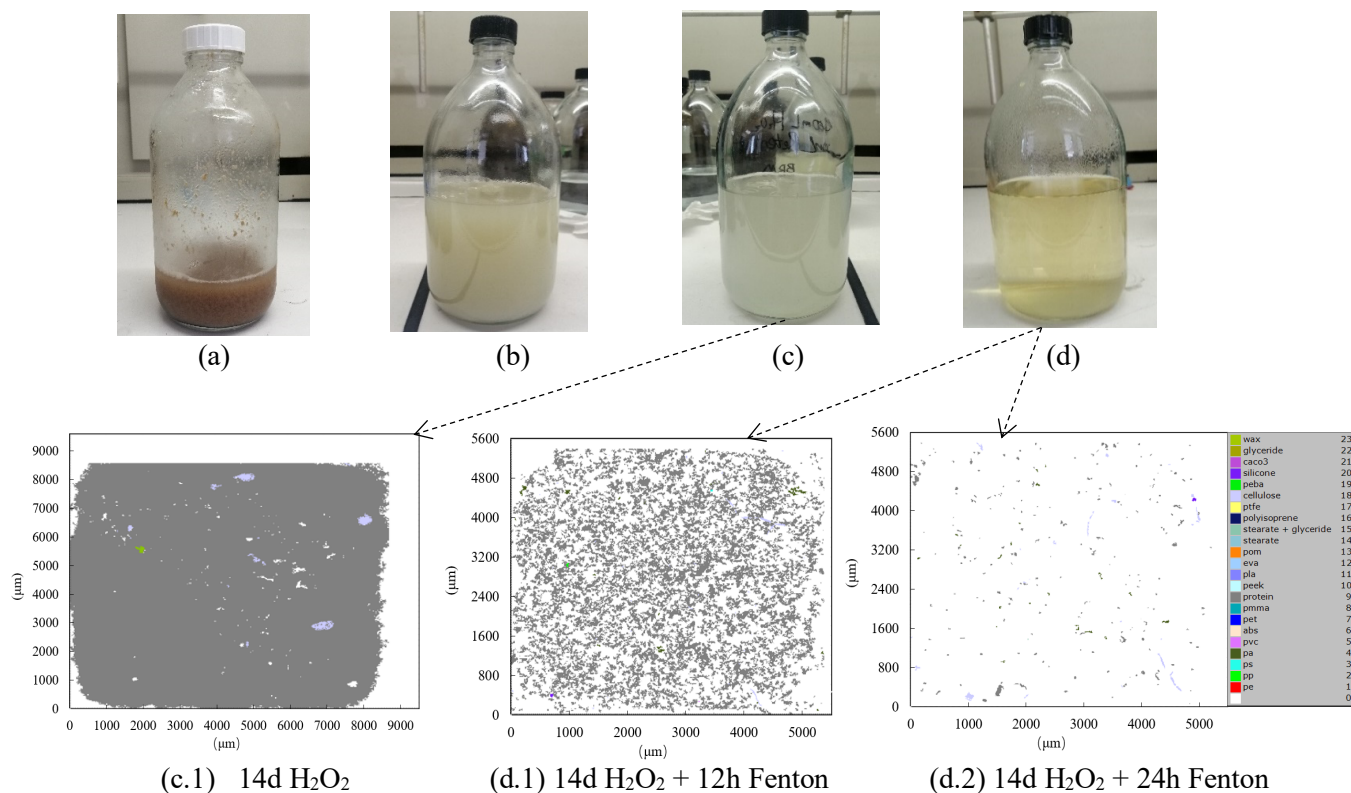
(a) 50 mL - 1 day digestion

(b) 50 mL - 7 days digestion

(c) 50 mL - 10 days digestion

293
 294 Figure 6 Visible survey of 50 mL secondary effluent (UF feed) from WWTP 4 on gold filter under (a) 1d
 295 digestion with H_2O_2 (b) 7d digestion with H_2O_2 (c) 10d digestion with H_2O_2 .

296 In view of raw wastewater, it contained higher concentrations in organic matters and particles
 297 compared to treated effluents, digestion by H_2O_2 ($V_{\text{sample}}:V_{H_2O_2} = 2:1$) was insufficient to
 298 completely oxidize the organics, even after 14 d reaction \rightarrow opaque and turbid (Figure 7 (a), (b)
 299 and (c)). Imaged by μ -FTIR, the main components identified in raw wastewater from WWTP5
 300 were proteins (Figure 7 (c.1)). As Fenton reagent could provide stronger digestion effects on
 301 organic-rich samples with less duration, and with fewer impacts on microplastic chemistry or size
 302 (Tagg et al., 2016), Fenton reagent ($V_{\text{sample}}:V_{\text{Fenton}}=4:1$) was added into the mixture after 14d H_2O_2
 303 oxidation and the pH was kept at 2.5-3.5 to avoid the oxidation of iron and iron flocs (Pilli et al.,
 304 2015). Sample after another 24h digestion by Fenton became much cleaner and transparent
 305 (Figure 7 (d)), and the complete decomposition of proteins after 24h Fenton reaction was observed
 306 by μ -FTIR images, as shown in Figure 7 (d.1) and (d.2).



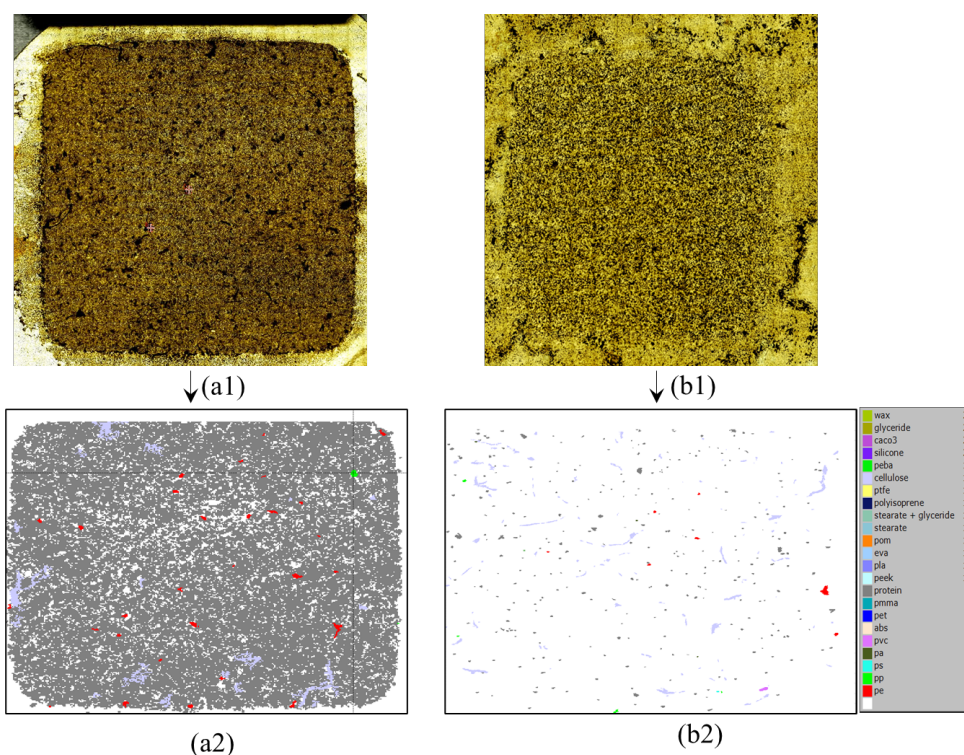
307
 308 Figure 7 Digestion process of raw wastewater from WWTP5 and the related spectral map of TPs on gold
 309 filters (a) without digestion (b) after 6d digestion with 30% H₂O₂ (c) after 14 d digestion with 30% H₂O₂
 310 (d) after 14 d digestion with H₂O₂ and 24h digestion with Fenton (c.1) 5 mL raw wastewater after 14d, H₂O₂
 311 digestion (d.1) 5 mL raw wastewater after 14d H₂O₂ and 12 h Fenton digestion (d.2) 15 mL raw wastewater
 312 after 14d H₂O₂ and 24h Fenton digestion $V_{\text{sample}}:V_{\text{H}_2\text{O}_2}=1:2$; $V_{\text{sample}}:V_{\text{Fenton}}=4:1$.

313 Therefore, it could be inferred that H₂O₂ was able to digest secondary effluents ($V_{\text{sample}}:V_{\text{H}_2\text{O}_2}$
 314 $=2:1$) with availability to digest organic matters, but not proteins and cellulose. Fenton as a stronger
 315 oxidative reagent showed effective decomposition on protein/cellulose-rich samples such as raw
 316 wastewaters. Therefore, sequentially digestion by H₂O₂ and Fenton for raw wastewater samples
 317 was suggested: H₂O₂ was firstly added ($V_{\text{sample}}:V_{\text{H}_2\text{O}_2} = 1:1$ to $1:2$) to partially oxidize samples
 318 within 3-14d, then Fenton was applied ($V_{\text{sample}}:V_{\text{Fenton}} = 4:1$ to $2:1$) to finalize the samples digestion
 319 within 12-36h.

320 3.4.2. Digestion of Seawater From SWTP With H₂O₂ and KOH

321 Seawater samples (seawater, Zeo-A outlet, Zeo-B outlet) digested by one-step H₂O₂ (>10d)
 322 resulted in little improvement on filtration. 15 mL net samples could completely foul the gold

323 filters (Figure 8 a1,a2). Since seawater might contain shellfish and plant/algae tissues, 10% (w/v)
 324 KOH was added to samples which could break down soft tissue and bivalve tissues (Thiele et al.,
 325 2019). However, some calcium hydroxide and magnesium hydroxide were generated after 10%
 326 KOH applied, resulting in white and turbid solution. Therefore, 10% H₂SO₄ was added drop by
 327 drop into the solution to eliminate the insoluble alkaline precipitation after KOH digestion.
 328 Afterwards, the visible survey of seawater samples became much clear for identification and
 329 quantification (Figure 8 (b1,b2)).



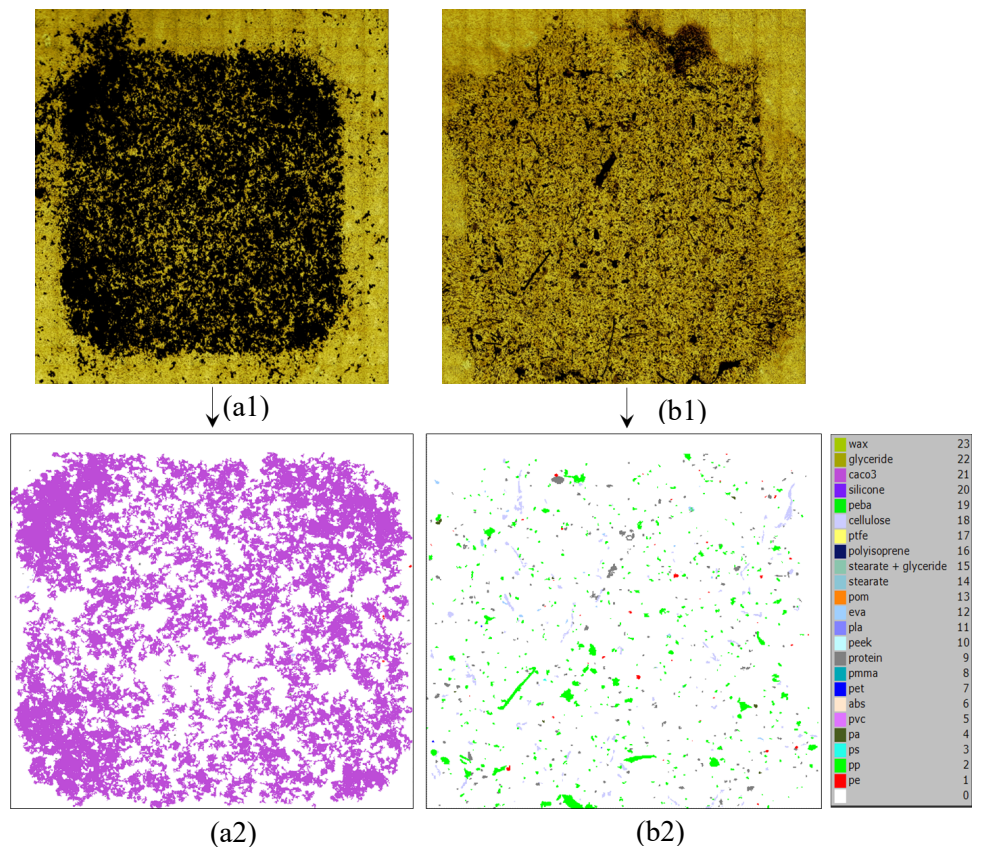
330
 331 Figure 8 Visible survey and Spectral map of seawater: (a1) (a2) represents the visible survey and spectral
 332 map of 15 mL seawater without digestion, respectively; (b1) (b2) represents the visible survey and spectral
 333 map of 37.5 mL seawater after KOH digestion, respectively.

334 3.4.3. Digestion of surface and underground water with acid and H₂O₂

335 Surface water and groundwater quality were significantly better than the samples from WWTPs
 336 and SWTP with transparent and less visible particles. Slight or none digestion was needed for these
 337 samples due to their components: Underground water from DWTP 1 needed some acid (10%
 338 H₂SO₄) to dissolve the CaCO₃, which formed white cake on gold-coated filter and covered MPs,
 339 shown in Figure 9 (a2). The components of surface water seem to be a bit more complex than

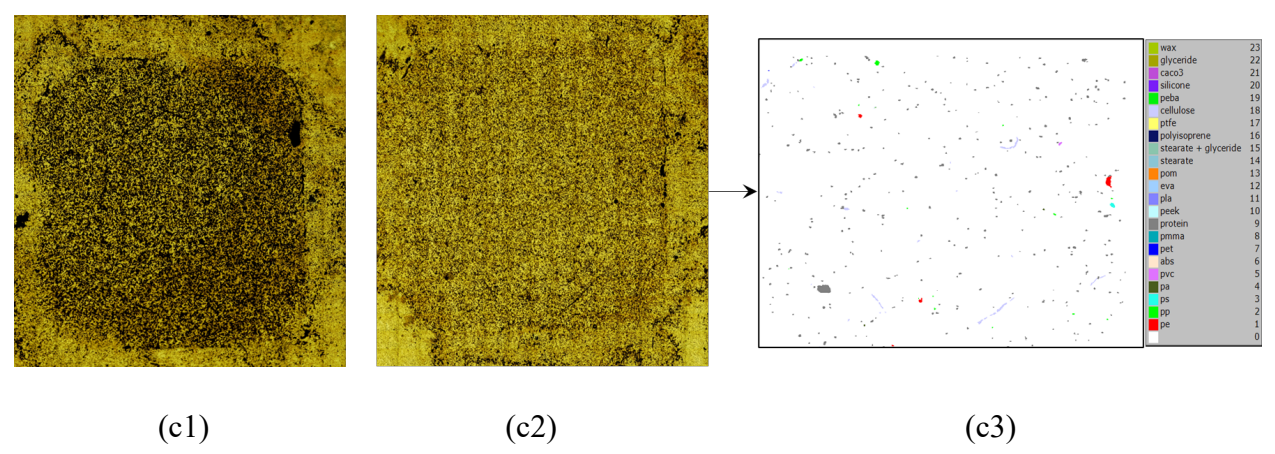
340 underground water, which contained CaCO₃, proteins, and cellulose (Figure 9 (c1,c2,c3)). A
 341 combined treatment by alkali (10% KOH) and acid (10% H₂SO₄) was applied for surface water
 342 from DWTP 3. Samples from DWTP 2 were purified enough to be filtrated through 5µm filters
 343 thus with no digestion requirement.

344



345

346



347

348

349 Figure 9 Visible survey and Spectral map of underground water (DWTP1) and surface water (DWTP3):
350 (a1) (a2) represent the visible survey and spectral map with TPs of 225 mL underground water without
351 digestion, respectively; (b1) (b2) represent the visible survey and spectral map with TPs of 485 mL sample
352 after acidification, respectively; (c1) represent the visible survey 30mL surface water digested with 10d
353 H₂O₂; (c2) (c3) represent the visible survey and spectral map in TPs of 30mL surface water digested with
354 10d H₂O₂ and 24h KOH.

355 3.4.4. Discussion on digestion improvement

356 Samples with digestion requirement were summarized in Table 3. Notably, samples without
357 digestion requirement were excluded, such as the UF permeates and DWTP2 samples. In fact, the
358 quality of samples without digestion were good enough to be filtrated directly all with turbidity
359 <1.0 NTU, TOC <6.0 mgC·L⁻¹, transparent, and non-visible suspended particles. Samples with
360 digestion requirement were discussed: In WWTPs, the decreased TOC and turbidity in secondary
361 effluents showed mild digesting method with 5-6 d H₂O₂, while raw wastewaters should be
362 digested with 7-14 d H₂O₂ and 12-24h Fenton. In SWTP, samples contained lower TOC (2.0 - 3.0
363 mgC·L⁻¹) but unignorable turbidity (1.3-6.3 NTU). The coupling of H₂O₂ and KOH were effective
364 for digestion and without further oxidation by Fenton probably due to the dissolved/undissolved
365 solids (salts, minerals, and tissues) (Al Dahaan et al., 2016). Samples from DWTPs had the best
366 qualities with lowest TOC (0.5-1.3 mgC·L⁻¹) and turbidity (0.34-1.2 NTU). DWTP2 samples need
367 no digestion demand. While DWTP 1 samples need slight oxidation by H₂O₂, and DWTP3 samples
368 need a further acidification, mainly due to the existences of proteins, cellulose, and CaCO₃.
369 Therefore, it was inferred that water quality could, but not decisively, influence the selection of
370 digestion especially on oxidative reactions; the composition of samples was considered as the main
371 factor for digestion. Normally, samples with higher TOC (>10 mgC·L⁻¹) and turbidity (>2 NTU)
372 usually need further oxidation compared to samples of better quality, while these samples of better
373 quality may still need slight oxidative, acidification, or alkalization process due to the dissolved
374 or undissolved particles.

375

376

377

Table 3 Water quality of digestion-required samples and the related digestion processes

Sources	Water types	TOC (mgC·L ⁻¹)	Turbidity (NTU)	Digestion method	Digestion process and duration	Main components identified	*V _{Net-max}	Number of replicates
WWTP 1 (Pharmaceutical)	Raw wastewater (MBR feed)	170–620	323–864	H ₂ O ₂ , Fenton	14d H ₂ O ₂ , 12h Fenton	Proteins, cellulose	14 mL	10
	Secondary effluent (MBR permeate)	36.5	17.4	H ₂ O ₂	6d		200 mL	5
WWTP 2	Raw wastewater	85.7	187	H ₂ O ₂ , Fenton	7d H ₂ O ₂ , 24h Fenton	Proteins, cellulose, stearate	40 mL	10
	Secondary effluent	4.9	0.18	H ₂ O ₂	5d	Proteins, cellulose	500 mL	4
WWTP 3	Raw wastewater	125.1	180	H ₂ O ₂ , Fenton	7d H ₂ O ₂ , 36h Fenton	Stearate, proteins, cellulose	45 mL	10
	Secondary effluent	9.9	10.7	H ₂ O ₂ , Fenton	7d H ₂ O ₂ , 24h Fenton	Proteins, cellulose	300 mL	4
WWTP 4	Raw wastewater	121.1	204	Fenton	24 h Fenton	Proteins, cellulose	60 mL	10
	Secondary effluent (UF feed)	6,627	1.8	H ₂ O ₂	5d		225 mL	4
Seawater treatment plant (SWTPs)	Seawater	-	-	H ₂ O ₂ , KOH (+acid)	5–6 d H ₂ O ₂ 1d KOH	Soft tissues (unidentified) and Minerals	37.5 mL	10
	Zeo-A outlet	2,322	1.3	-	-		200 mL	8
	Zeo-B outlet	2,096	4.8	H ₂ O ₂ , KOH (+acid)	5–6 d H ₂ O ₂ 1d KOH		42 mL	10
	Old UF feed	-	6.3	H ₂ O ₂ , KOH (+acid)	10d H ₂ O ₂ 1d KOH		14 mL	10
	New UF feed	2,896	3.4	H ₂ O ₂	7d		70 mL	5
DWTP 1	Underground water	0.59	0.7	Acid	2h	CaCO ₃	485 mL	3
	Primary effluent	0.62	1.2	H ₂ O ₂	2d	Proteins	150 mL	4
DWTP3	Surface water	1.3	0.34	H ₂ O ₂ , Acid	14 d H ₂ O ₂	Proteins, CaCO ₃ , cellulose	30 mL	10
	Sedimentation outlet	1.2	0.68	H ₂ O ₂ , Acid	7–14 d H ₂ O ₂		100 mL	5

379 *V_{Net-max} represents the max volume of the samples passing through the gold filters in this study

380
 381 In view of digesting duration, oxidation by H₂O₂ needed the longest duration (2-14d) compared
 382 to Fenton oxidation (12-36h), alkalization (\leq 24h), and acidification (<1h), thus 14 d by H₂O₂
 383 was considered as a turning timepoint where stronger oxidation was necessary. To shorten
 384 digestion duration, larger dosage of chemicals, increased concentration, or higher temperature
 385 could be applied (Hurley et al., 2018; Prata et al., 2019). With samples enriched in organics, the

386 pre-digesting process by H₂O₂ could be partially shortened (to 5-7d) and followed by Fenton
387 oxidation. Notably, improvements by heating and digestion duration, and higher concentration,
388 particularly by alkalization and acidification, could increase the risks on damage of microplastic
389 properties, such as decolorization, oxidation, or even degradation (Hurley et al., 2018; Schirinzi et
390 al., 2020). Regarding negative effects of digestion, some studies demonstrated the partial
391 degradation (<18% of recovery) of PC and PET by 10 % KOH when increasing temperature to
392 60 °C (Karami et al., 2017), and some polymers were founded to be damaged with concentrated
393 acid (e.g. ≥ 69 % HNO₃) under high temperatures (T ≥ 50 °C) (Schirinzi et al., 2020). Actually,
394 most plastic polymers were impervious to digestion by 10 % KOH under controlled temperature
395 (≤ 60 °C) and digestion duration (≤ 24 h) (F. Li et al., 2018), and reducing acid concentration would
396 protect most polymers (e.g. PA, PC, PE, PET, PP, PS and PVC) from breaking down at room
397 temperature (Schirinzi et al., 2020). To minimize damage to microplastics, this study was
398 conducted under room temperature throughout all digestion processes, and the digestion duration
399 by alkalization were controlled within 24h, and acidification was usually applied before filtration
400 immediately. More efforts on optimization of digesting duration can be made in recent future.

401 3.5. Reliability of the Method

402 To evaluate the reliability of the μ -FTIR coupled with siMPle detection method , nine criteria
403 described by Koelmans et al. (2019), including sampling method, sample size, processing and
404 storage, laboratory preparation and clean air conditions, negative and positive controls, sample
405 treatment and polymer identification were self-assessed (Table 4). The details about each criteria
406 were listed in Table S3 SI . The highest reliability is obtained for the highest score. On negative
407 controls, MPs in air and in various types of rinsing water were detected for ≥ 3 replicates (section
408 3.2), and rinsing water (UP and filtrated ethanol) was evaluated to be ignorable (<2 MPs) both
409 used for lab samples and field samples (DWTPs, WWTPs, and SWTP); The uncertainty was the
410 control not always detected before each type of water. Therefore, the negative control should be
411 scored at least for 1, and probably for 2. Relatively, the PE solution was detected as the positive
412 control to evaluate μ -FTIR and siMPle method, resulted with qualified MP types, and with
413 dimensions (10-150 μ m) and shapes (microspheres) consistent with manufactures, while the
414 recovery rate was undetectable, resulting in 1 score for positive control. Compared to Koelmans

415 et al. (2019) scoring 11.5 for treated tap water, 12.5 for DWTP water, 7.9 for surface water, and
 416 7.3 for wastewater, this study obtained equivalent score for tap water (11-12), higher scores for
 417 surface waters (11-13) and wastewaters (13-14). To be more relevant, four other recent studies (<3
 418 years) were also evaluated for comparison. The scores (11-14) in our study still ranked in front
 419 position. Particularly, the comparative detection on drinking water by Kirstein et al. (2021) and on
 420 potable water by Johnson et al. (2020) also used μ -FTIR for analysis. Therefore, the qualified
 421 scores in this study and the proves by studies using μ -FTIR both demonstrated the reliability of
 422 this proposed approach.

423 Table 4 Self-Assessment of microplastic identification and quantification method in this work and the
 424 recent studies (Johnson et al., 2020; Kirstein et al., 2021; Ourgaud et al., 2022; Primpke et al., 2020b)

Type of samples	Criteria									Total score
	Sampling methods	Sample size	Sample process and storage	Lab preparation	Clean air conditions	Negative control	Positive control	Sample treatment	Polymer identification	
Seawater (surface)	1	1	1	2	1	1-2	1	2	2	12-13
Wastewater	2	1	1	2	1	1-2	1	2	2	13-14
Surface water/ groundwater	1	0	1	2	1	1-2	1	2	2	11-12
Tap water	1	0	1	2	1	1-2	1	2	2	11-12
Marine water (Ourgaud et al., 2022)	2	1	2	1	1	1	1	1	1	11
Various waters (Primpke et al., 2020)	1	0	0	0	0	1	1	0	1	4
Drinking water (Kirstein et al., 2021)	2	2	1	1	1	2	1	1	2	13
Potable water (Johnson et al., 2020)	2	2	1	1	1	2	2	1	2	14

425

426

427 4. Conclusion

428 This study aims to develop an independent method approach for the identification and
429 quantification of microplastics in different water samples (sea, fresh and wastewater). After
430 comparison between different rinsing waters/solution, ultrapure water and filtrated ethanol were
431 selected based on the lowest number of MPs found. Synthetic PE particles were used to verify the
432 type and sizes obtained by μ -FTIR focal-plane-array coupled with SiMPle software. A
433 proportional relationship was obtained between the number of PE particles and filtrated volume
434 even if filtrating the same and highest volume possible of the sample is preferable. The
435 pretreatment of samples (i.e., digestion) was demonstrated to be crucial. In summary, organic
436 matters such as proteins and cellulose can be oxidized by H_2O_2 or Fenton, some salts such as
437 $CaCO_3$, stearate can be digested by acids, and soft tissues or muscle can be digested with KOH.
438 Normally, samples with higher TOC, turbidity, and higher suspended solids need stronger
439 digestion. Some ranges of these parameters are given to estimate the digestion mode. The water
440 quality can give some reference to the level of digestion, but it is not the decisive factor and there
441 is no specific relationship between the water quality and digestion levels (method, duration,
442 dosage). For examples, the TOC and turbidity among tertiary treated water, seawater, and surface
443 water are very similar and all of them are in quite low values, but the tertiary treated effluents are
444 all good enough to be filtrated more than 500 mL at once without digestion, while the others cannot.
445 Therefore, it is necessary to know the real components in the samples and choose the effective
446 methods. The concentration of chemicals and contact time are both controlled in acceptable ranges
447 to have no or very few effects on microplastic properties, according to the research experiences
448 and literature.

449 Finally, considering the recent literature, rigorous detection process and high-precision
450 analytical methods to obtain the number, size and type of microplastics by μ -FTIR focal-plane-
451 array imaging were developed in this Part I and will be used in Part II to assess the efficiency of
452 (membrane) treatment processes to remove MPs in very different water treatment plants.

453

454 5. Acknowledgment

455 The authors would like to warmly thank Alexandre Michelet and Jean-Philippe Mélis from
456 PerkinElmer for provisioning them with the FTIR microscope and for helping to use it, Stéphanie
457 Lebarillier (LCE lab) for the technical support, the ECCOREV Research Federation (FR3098) and
458 ITEM Research and Teaching Institute from Aix-Marseille University for their financial support.

459

460

461 6. References

- 462 Al Dahaan, S., Al-Ansari, N., Knutsson, S., 2016. Influence of Groundwater Hypothetical Salts on
463 Electrical Conductivity Total Dissolved Solids. *Engineering* 8, 823–830.
- 464 Anger, P.M., von der Esch, E., Baumann, T., Elsner, M., Niessner, R., Ivleva, N.P., 2018. Raman
465 microspectroscopy as a tool for microplastic particle analysis. *TrAC Trends Anal. Chem.* 109,
466 214–226. <https://doi.org/10.1016/j.trac.2018.10.010>
- 467 Campanale, Massarelli, Savino, Locaputo, Uricchio, 2020. A Detailed Review Study on Potential Effects
468 of Microplastics and Additives of Concern on Human Health. *Int. J. Environ. Res. Public. Health*
469 17, 1212. <https://doi.org/10.3390/ijerph17041212>
- 470 Frias, J.P.G.L., Nash, R., 2019. Microplastics: Finding a consensus on the definition. *Mar. Pollut. Bull.*
471 138, 145–147. <https://doi.org/10.1016/j.marpolbul.2018.11.022>
- 472 Gonzalez-Torres, A., Rich, A.M., Marjo, C.E., Henderson, R.K., 2017. Evaluation of biochemical algal
473 floc properties using Reflectance Fourier-Transform Infrared Imaging. *Algal Res.* 27, 345–355.
474 <https://doi.org/10.1016/j.algal.2017.09.017>
- 475 Hong, Y., Oh, J., Lee, I., Fan, C., Pan, S.-Y., Jang, M., Park, Y.-K., Kim, H., 2021. Total-organic-carbon-
476 based quantitative estimation of microplastics in sewage. *Chem. Eng. J.* 423, 130182.
477 <https://doi.org/10.1016/j.cej.2021.130182>
- 478 Hurley, R.R., Lusher, A.L., Olsen, M., Nizzetto, L., 2018. Validation of a Method for Extracting
479 Microplastics from Complex, Organic-Rich, Environmental Matrices. *Environ. Sci. Technol.* 52,
480 7409–7417. <https://doi.org/10.1021/acs.est.8b01517>
- 481 Jambeck, J.R., Geyer, R., Wilcox, C., Siegler, T.R., Perryman, M., Andrady, A., Narayan, R., Law, K.L.,
482 2015. Plastic waste inputs from land into the ocean. *Science* 347, 768–771.
483 <https://doi.org/10.1126/science.1260352>
- 484 Johnson, A.C., Ball, H., Cross, R., Horton, A.A., Jürgens, M.D., Read, D.S., Vollertsen, J., Svendsen, C.,
485 2020. Identification and Quantification of Microplastics in Potable Water and Their Sources
486 within Water Treatment Works in England and Wales. *Environ. Sci. Technol.* 54, 12326–12334.
487 <https://doi.org/10.1021/acs.est.0c03211>
- 488 Karami, A., Golieskardi, A., Choo, C.K., Romano, N., Ho, Y.B., Salamatinia, B., 2017. A high-
489 performance protocol for extraction of microplastics in fish. *Sci. Total Environ.* 578, 485–494.
490 <https://doi.org/10.1016/j.scitotenv.2016.10.213>
- 491 Karlsson, T.M., Kärman, A., Rotander, A., Hassellöv, M., 2020. Comparison between manta trawl and in
492 situ pump filtration methods, and guidance for visual identification of microplastics in surface
493 waters. *Environ. Sci. Pollut. Res.* 27, 5559–5571. <https://doi.org/10.1007/s11356-019-07274-5>
- 494 Kirstein, I.V., Hensel, F., Gomiero, A., Iordachescu, L., Vianello, A., Wittgren, H.B., Vollertsen, J., 2021.
495 Drinking plastics? – Quantification and qualification of microplastics in drinking water

496 distribution systems by μ FTIR and Py-GCMS. *Water Res.* 188, 116519.
497 <https://doi.org/10.1016/j.watres.2020.116519>

498 Koelmans, A.A., Mohamed Nor, N.H., Hermsen, E., Kooi, M., Mintenig, S.M., De France, J., 2019.
499 Microplastics in freshwaters and drinking water: Critical review and assessment of data quality.
500 *Water Res.* 155, 410–422. <https://doi.org/10.1016/j.watres.2019.02.054>

501 Lebreton, L.C.M., van der Zwet, J., Damsteeg, J.-W., Slat, B., Andrady, A., Reisser, J., 2017. River
502 plastic emissions to the world's oceans. *Nat. Commun.* 8, 15611.
503 <https://doi.org/10.1038/ncomms15611>

504 Li, F., Li, Fuyun, Hou, X., Luo, X., Tu, H., Zou, Y., Sun, C., Shi, M., Zheng, H., 2018. Comparison of six
505 digestion methods on fluorescent intensity and morphology of the fluorescent polystyrene beads.
506 *Mar. Pollut. Bull.* 131, 515–524. <https://doi.org/10.1016/j.marpolbul.2018.04.056>

507 Li, J., Liu, H., Paul Chen, J., 2018. Microplastics in freshwater systems: A review on occurrence,
508 environmental effects, and methods for microplastics detection. *Water Res.* 137, 362–374.
509 <https://doi.org/10.1016/j.watres.2017.12.056>

510 Mintenig, S.M., Kooi, M., Erich, M.W., Primpke, S., Redondo- Hasselerharm, P.E., Dekker, S.C.,
511 Koelmans, A.A., van Wezel, A.P., 2020. A systems approach to understand microplastic
512 occurrence and variability in Dutch riverine surface waters. *Water Res.* 176, 115723.
513 <https://doi.org/10.1016/j.watres.2020.115723>

514 Nizzetto, L., Langaas, S., Futter, M., 2016. Pollution: Do microplastics spill on to farm soils? *Nature* 537,
515 488–488. <https://doi.org/10.1038/537488b>

516 Nobre, C.R., Santana, M.F.M., Maluf, A., Cortez, F.S., Cesar, A., Pereira, C.D.S., Turra, A., 2015.
517 Assessment of microplastic toxicity to embryonic development of the sea urchin *Lytechinus*
518 *variegatus* (Echinodermata: Echinoidea). *Mar. Pollut. Bull.* 92, 99–104.
519 <https://doi.org/10.1016/j.marpolbul.2014.12.050>

520 Ourgaud, M., Phuong, N.N., Papillon, L., Panagiotopoulos, C., Galgani, F., Schmidt, N., Fauvelle, V.,
521 Brach-Papa, C., Sempéré, R., 2022. Identification and Quantification of Microplastics in the
522 Marine Environment Using the Laser Direct Infrared (LDIR) Technique. *Environ. Sci. Technol.*
523 56, 9999–10009. <https://doi.org/10.1021/acs.est.1c08870>

524 Pilli, S., Yan, S., Tyagi, R.D., Surampalli, R.Y., 2015. Overview of Fenton pre-treatment of sludge
525 aiming to enhance anaerobic digestion. *Rev. Environ. Sci. Biotechnol.* 14, 453–472.
526 <https://doi.org/10.1007/s11157-015-9368-4>

527 Prata, Joana Correia, da Costa, J.P., Duarte, A.C., Rocha-Santos, T., 2019. Methods for sampling and
528 detection of microplastics in water and sediment: A critical review. *TrAC Trends Anal. Chem.*
529 110, 150–159. <https://doi.org/10.1016/j.trac.2018.10.029>

530 Prata, Joana C., da Costa, J.P., Girão, A.V., Lopes, I., Duarte, A.C., Rocha-Santos, T., 2019. Identifying a
531 quick and efficient method of removing organic matter without damaging microplastic samples.
532 *Sci. Total Environ.* 686, 131–139. <https://doi.org/10.1016/j.scitotenv.2019.05.456>

533 Prata, J.C., Manana, M.J., da Costa, J.P., Duarte, A.C., Rocha-Santos, T., 2020. What Is the Minimum
534 Volume of Sample to Find Small Microplastics: Laboratory Experiments and Sampling of Aveiro
535 Lagoon and Vouga River, Portugal. *Water* 12, 1219. <https://doi.org/10.3390/w12041219>

536 Primpke, S., Cross, R.K., Mintenig, S.M., Simon, M., Vianello, A., Gerdts, G., Vollertsen, J., 2020a.
537 Toward the Systematic Identification of Microplastics in the Environment: Evaluation of a New
538 Independent Software Tool (siMPle) for Spectroscopic Analysis. *Appl. Spectrosc.* 74, 1127–
539 1138. <https://doi.org/10.1177/0003702820917760>

540 Primpke, S., Godejohann, M., Gerdts, G., 2020b. Rapid Identification and Quantification of Microplastics
541 in the Environment by Quantum Cascade Laser-Based Hyperspectral Infrared Chemical Imaging.
542 *Environ. Sci. Technol.* 54, 15893–15903. <https://doi.org/10.1021/acs.est.0c05722>

543 Radford, F., M. Zapata-Restrepo, L., A. Horton, A., D. Hudson, M., J. Shaw, P., D. Williams, I., 2021.
544 Developing a systematic method for extraction of microplastics in soils. *Anal. Methods* 13, 1695–
545 1705. <https://doi.org/10.1039/D0AY02086A>

546 Ragusa, A., Svelato, A., Santacroce, C., Catalano, P., Notarstefano, V., Carnevali, O., Papa, F.,
547 Rongioletti, M.C.A., Baiocco, F., Draghi, S., D'Amore, E., Rinaldo, D., Matta, M., Giorgini, E.,
548 2021. Plasticenta: First evidence of microplastics in human placenta. *Environ. Int.* 146, 106274.
549 <https://doi.org/10.1016/j.envint.2020.106274>

550 Rillig, M.C., 2012. Microplastic in Terrestrial Ecosystems and the Soil? *Environ. Sci. Technol.* 46, 6453–
551 6454. <https://doi.org/10.1021/es302011r>

552 Schirinzi, G.F., Pedà, C., Battaglia, P., Laface, F., Galli, M., Bainsi, M., Consoli, P., Scotti, G., Esposito,
553 V., Faggio, C., Farré, M., Barceló, D., Fossi, M.C., Andaloro, F., Romeo, T., 2020. A new
554 digestion approach for the extraction of microplastics from gastrointestinal tracts (GITs) of the
555 common dolphinfish (*Coryphaena hippurus*) from the western Mediterranean Sea. *J. Hazard.*
556 *Mater.* 397, 122794. <https://doi.org/10.1016/j.jhazmat.2020.122794>

557 Sherrington, C., Darrah, C., Hann, S., Cole, G., Corbin, M., 2016. Study to support the development of
558 measures to combat a range of marine litter sources: Report for European Commission DG
559 Environment. Eunomia.

560 Sherrington, Chris, Darrah, C., Hann, S., Cordle, M., 2016. Study to Support the Development of
561 Measures to Combat a Range of Marine Litter Sources. Eunomia.

562 Shim, W.J., Hong, S.H., Eo, S.E., 2017. Identification methods in microplastic analysis: a review. *Anal.*
563 *Methods* 9, 1384–1391. <https://doi.org/10.1039/C6AY02558G>

564 Simon, M., van Alst, N., Vollertsen, J., 2018. Quantification of microplastic mass and removal rates at
565 wastewater treatment plants applying Focal Plane Array (FPA)-based Fourier Transform Infrared
566 (FT-IR) imaging. *Water Res.* 142, 1–9. <https://doi.org/10.1016/j.watres.2018.05.019>

567 Stock, F., Kochleus, C., Bänisch-Baltruschat, B., Brennholt, N., Reifferscheid, G., 2019. Sampling
568 techniques and preparation methods for microplastic analyses in the aquatic environment – A
569 review. *TrAC Trends Anal. Chem.* 113, 84–92. <https://doi.org/10.1016/j.trac.2019.01.014>

570 Sun, J., Dai, X., Wang, Q., van Loosdrecht, M.C.M., Ni, B.-J., 2019. Microplastics in wastewater
571 treatment plants: Detection, occurrence and removal. *Water Res.* 152, 21–37.
572 <https://doi.org/10.1016/j.watres.2018.12.050>

573 Sussarellu, R., Suquet, M., Thomas, Y., Lambert, C., Fabioux, C., Pernet, M.E.J., Goïc, N.L., Quillien,
574 V., Mingant, C., Epelboin, Y., Corporeau, C., Guyomarch, J., Robbens, J., Paul-Pont, I., Soudant,
575 P., Huvet, A., 2016. Oyster reproduction is affected by exposure to polystyrene microplastics.
576 *Proc. Natl. Acad. Sci.* 113, 2430–2435. <https://doi.org/10.1073/pnas.1519019113>

577 Tagg, A., Sapp, M., Harrison, J., Ojeda, J., 2015. Identification and Quantification of Microplastics in
578 Wastewater Using Focal Plane Array-Based Reflectance Micro-FT-IR Imaging. *Anal. Chem.* 87,
579 6032–6040. <https://doi.org/10.1021/acs.analchem.5b00495>

580 Tagg, A.S., Harrison, J.P., Ju-Nam, Y., Sapp, M., Bradley, E.L., Sinclair, C.J., Ojeda, J.J., 2016. Fenton's
581 reagent for the rapid and efficient isolation of microplastics from wastewater. *Chem. Commun.*
582 53, 372–375. <https://doi.org/10.1039/C6CC08798A>

583 Tagg, A.S., Sapp, M., Harrison, J.P., Ojeda, J.J., 2015. Identification and Quantification of Microplastics
584 in Wastewater Using Focal Plane Array-Based Reflectance Micro-FT-IR Imaging. *Anal. Chem.*
585 87, 6032–6040. <https://doi.org/10.1021/acs.analchem.5b00495>

586 Thiele, C.J., Hudson, M.D., Russell, A.E., 2019. Evaluation of existing methods to extract microplastics
587 from bivalve tissue: Adapted KOH digestion protocol improves filtration at single-digit pore size.
588 *Mar. Pollut. Bull.* 142, 384–393. <https://doi.org/10.1016/j.marpolbul.2019.03.003>

589 Yang, J.-Q., Li, Z.-L., Wu, B., Jin, Y.-R., Cao, D., Nan, J., Chen, X.-Q., Liu, W.-Z., Gao, S.-H., Wang,
590 A.-J., 2022. Insights into the influence on 2,4,6-Trichlorophenol microbial reductive
591 dechlorination process by exposure to microplastics. *J. Hazard. Mater.* 129978.
592 <https://doi.org/10.1016/j.jhazmat.2022.129978>

593 Zheng, Y., Li, J., Sun, C., Cao, W., Wang, M., Jiang, F., Ju, P., 2021. Comparative study of three
594 sampling methods for microplastics analysis in seawater. *Sci. Total Environ.* 765, 144495.
595 <https://doi.org/10.1016/j.scitotenv.2020.144495>

